# Electrochemical Sensing Platform Based on Polyelectrolyte−Surfactant Supramolecular Assemblies Incorporating Carbon Nanotubes

M. Lorena Cortez,[†,‡] Marcelo Ceolín,[§] Omar Azzaroni,[§] and Fernando Battaglini*[,†]

[†]INQUIMAE, Departamento Química Inorgánica, Analítica y Química Física, and [‡]PINMATE, Departamento de Industrias, Facultad de Ciencias Exactas y Naturales, Universidad de Buenos Aires, Ciudad Universitaria, Pabellón 2, C1428EHA Buenos Aires, Argentina

[§]Instituto de Investigaciones Fisicoquímicas Teóricas y Aplicadas, Departamento de Química, Facultad de Ciencias Exactas, Universidad Nacional de La Plata, CONICET, La Plata, Buenos Aires, Argentina

ABSTRACT: The characterization and application of a poly-electrolyte−surfactant supramolecular assembly formed by poly-(allylamine) and dodecyl sulfate (PA−DS) on a screen-printed graphite electrode for the preparation of electrochemical sensing platforms are presented. The system was characterized by X-ray reflectometry (XRR) and grazing-incidence small-angle X-ray scattering (GISAXS) and tested with four benchmark electrochemical probes undergoing different electron-transfer mechanisms on carbon: ferrocyanide, hexaammineruthenium, ascorbic acid, and dopamine. The polyelectrolyte acts as a scaffold favoring the incorporation of the ferrocyanide, an ion oppositely charged to poly(allylamine). Also, its ability to incorporate carbon nanotubes (CNT) is presented. The composite material PA−DS−CNT is able to electrocatalyze the oxidation of dopamine, allowing its detection at micromolar levels in the presence of 100 times higher concentrations of ascorbate and it is shown to be stable, while XRR and GISAXS results confirm a lamellar structure with well-defined domains, not perturbed by the presence of the CNT. The dispersion is easily prepared in aqueous solution and could facilitate the processing of the CNT with an efficient loading and yielding a more robust carbon-based material for sensing applications.
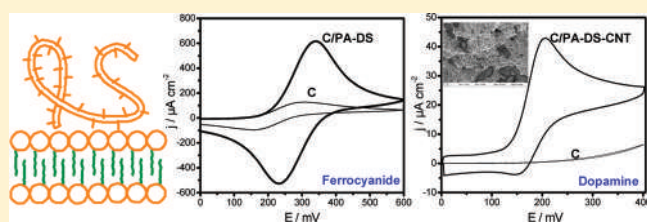
$\mathbf{S}$urfactants are amphiphilic molecules containing a hydrophilic head and a hydrophobic tail; they are applied in electrochemistry to improve electrode/solution interface properties.[1−3] They have been demonstrated to be very helpful in electrocatalysis by forming ionic micelles or monolayers on electrode surfaces. Also, they are able to efficiently disperse nanoparticles commonly used in electrocatalysis.[4−7] On the other hand, they cannot be efficiently adsorbed on any type of surface and the ability to be further modified is practically nil, since they are generally formed by an alkyl chain and an ionic group with no chance to be modified by mild methods.

On the other hand, several weak polyelectrolytes, such as those containing carboxylate [e.g., poly(acrylic acid)] or amino moieties [e.g., poly(allylamine)], have been used to introduce functional groups on electrodes, allowing further modifications.[8−10] However, the ability of these materials to stand by themselves on a surface is limited to electrostatic interactions in self-assembled systems forming multilayer films, or by cross-linking reactions forming hydrogels. Particularly, polyelectrolyte multilayer films have the advantage of controlling the molecular architecture;[11,12] in spite of this, in many cases no clear advantages are perceived when they are applied to sensor construction. Moreover, even though the self-assembled process can be automatized, it is a time-consuming procedure if several layers are needed.

Polyelectrolyte−surfactant polymers are complexes of charged polymeric chains (polyelectrolytes) and oppositely charged small amphiphilic molecules (surfactants). Such complexes combine in unique ways the properties of polyelectrolyte with those of low molecular weight amphiphiles. The polyelectrolyte components can provide, for instance, mechanical strength and thermal stability, while the surfactants retain their tendency to assemble in layered structures.[13,14] They are able to form stable colloidal suspensions in water[15] and they can be completely dissolved in organic solvent,[13,16] allowing easier handling and a very stable structure after drying.

Using all this knowledge, we decided to explore the characteristics of a polyelectrolyte−surfactant complex formed by a poly-(allylamine) and dodecyl sulfate as a supremolecular assembly on screen-printed graphite electrodes. Graphite shows several advantages such as low cost, wide potential window, and relatively inert electrochemistry, making it an ideal substrate for sensors construction. Electrodes modified with this matrix were tested with four benchmark electrochemical probes—ferrocyanide,

hexaammineruthenium, ascorbic acid, and dopamine—in order to understand its influence on different electron-transfer processes[17] and with carbon nanotubes, a well-known electrocatalyst, incorporated in the complex matrix. The film structure was characterized by X-ray reflectometry (XRR), grazing-incidence small-angle X-ray scattering (GISAXS), and contact angle analysis.

Among the most interesting features found in these new modified electrodes is the formation of stable films able to efficiently retain negatively charged ions and to disperse carbon nanotubes (CNT). The CNT-modified electrodes electrocatalyze the oxidation of dopamine, allowing its detection at micromolar levels in the presence of 100 times higher concentrations of ascorbate. The presented supramolecular assembly incorporating carbon nanotubes can be regarded as a more robust carbon-abased material for sensor construction.

■ EXPERIMENTAL SECTION

Reagents and Materials. Sodium dodecyl sulfate (SDS) was from Kodak, and poly(allylamine) (PA) was from Sigma—Aldrich (MW 65 000). Multiwall carbon nanotubes were from Timesnano (OD 10—20 nm; length ~30 μm, —COOH content 2.00 wt %, purity >95 wt %), and they were used as received. All other reagents were analytical-grade. Graphite screen-printed electrodes were constructed as previously described.[18]

PA—DS Composite Material. PA was dissolved in water to a final concentration of 0.18 mM, and the pH of the solution was adjusted to 7.0 with HCl. PA (100 μL of 0.18 mM solution) was mixed with 200 μL of 35 mM SDS aqueous solution; immediately a white dispersion was formed that is stable throughout the time. All the experiments were carried out with this mixture otherwise stated.

PA—DS—CNT Composite Material. CNT (3 mg) was suspended in 2 mL of 35 mM SDS aqueous solution, and 200 μL of this dispersion was mixed with 100 μL of 0.18 mM PA (adjusted to pH 7.0 with HCl).

Modified Electrodes. *PA—DS Electrodes.* Graphite electrodes (0.38 cm^2) were modified by applying 5 μL of the PA—DS dispersion and left to cast for at least 2 h. The modified electrodes prepared for the experiment shown in Figure 4 were prepared from a dispersion produced by the mixture of 200 μL of 3 mM PA (adjusted to pH 7.0) with 200 μL of 35 mM SDS aqueous solution. Graphite electrodes (0.38 cm^2) were modified by applying 5 μL of this mixture. In both cases, film thickness was measured by a stylus profilometry technique with a Veeco Dektak 150 surface profiler.

PA—DS—CNT Electrodes. The dispersion containing CNT (5 μL) was applied on a graphite electrode (0.38 cm^2) and left to cast for more than 2 h.

Measurements. Electrochemical experiments were carried out on a purpose-built potentiostat (TEQ-02). The system consisted of a working electrode, a platinum mesh counter-electrode, and an Ag|AgCl reference electrode. Cyclic voltammetries were carried out in 50 mM phosphate buffer (pH = 7, 0.2 M KNO$_3$) unless otherwise stated. Differential pulse voltammetries were carried out at a scan rate of 10 mV·s^{-1}, with 50 mV pulse amplitude, 25 ms pulse width, and 500 ms pulse period.

Micrographs. Micrographs were taken with a field emission scanning electron microscope (FESEM) Zeiss DSM 982 Gemini at the Advanced Center for Microscopies (CMA, Universidad de Buenos Aires).

Light Scattering Measurements. Dynamic light scattering (DLS) measurements were carried out in a Brookhaven particle size analyzer model 90plus, provided with a 28 mW laser (657 nm). Measurements were carried out at a fixed scattering angle of 90°. Samples were contained in a disposable polystyrene cell.

Contact Angle. Advancing contact angle of water experiments were carried out in a KSV Cam200 optical contact angle meter.

X-ray Reflectometry and Grazing-Incidence Small-Angle X-ray Scattering Measurements. X-ray reflectometry (XRR) and grazing-incidence small-angle X-ray scattering (GISAXS) measurements were performed at the D10A-XRD2 line of Laboratório Nacional de Luz Síncrotron (LNLS, Campinas, Brazil). A monochromatic beam of 7709 eV ($\lambda = 1.608$ Å) was used to perform both XRR and GISAXS experiments. Si(100) wafers were used as support substrates and were pretreated before coating. They were rinsed with acetone and dried with argon blowing before being coated. Thin polymer films were prepared by spin-coating a 50 μL portion of PA—DS or PA—DS—CNT dispersion by use of a commercial spin coater (Laurell WS-400B).

■ RESULTS

Colloidal Suspension. Poly(allylamine) (PA) is a weak ationic polyelectrolyte of basic nature, with a reported pK_a of 9.7.[19] It is able to readily solubilize at neutral pH given a fully positively charged polymer. When this solution is mixed with sodium dodecyl sulfate, a stable particle dispersion is produced, having an effective diameter of 281 ± 11 nm. An interesting characteristic of this colloidal system is the simplicity of the particle preparation: the addition of SDS produces a stable colloidal system, as long the pH of the PA is below 10; considering the pK_a of PA, at least half of the amino groups have to be protonated to induce the formation of a colloidal suspension.

PA—DS Films. The dispersion can be easily handled and applied onto a screen-printed graphite surface, producing a stable coating after solvent evaporation. The exposition of the system to a drop of water gives a contact angle of (85 ± 5)°, showing a more hydrophobic behavior than that observed when PA is forming the outermost layer in structures constructed layer by layer in combination with poly(styrenesulfonate),[20] where a value of (46 ± 1)° was reported, suggesting a strong interaction between the oppositely charged groups, leaving exposed to the solution the alkyl moieties of the composite material.

The structure of the film was further characterized by specular X-ray reflectivity analysis and grazing-incidence small-angle X-ray scattering measurements. They were carried out with synchrotron radiation sources to investigate the mesostructural organization of the PA—DS and PA—DS—CNT films formed on solid surfaces, Si(100). Figure 1a shows the X-ray reflectivity data for the PA—DS thin film. The presence of sharp Bragg peaks up to the third order indicates highly oriented lamellar structure. From the Bragg peak positions, a lamellar spacing of 3.96 ± 0.06 nm for the PA—DS system can be deduced. The simplest lamellar nanostructure of a polyelectrolyte—surfactant complex is a microphase-separated model consisting of an ionic phase and a nonionic phase. The ionic phase contains the polyelectrolyte chains and the ionic head groups of the surfactants, while the nonionic phase contains the hydrophobic moieties such as alkyl chains (Figure 1, bottom).[21] The repeat unit of a lamellar system
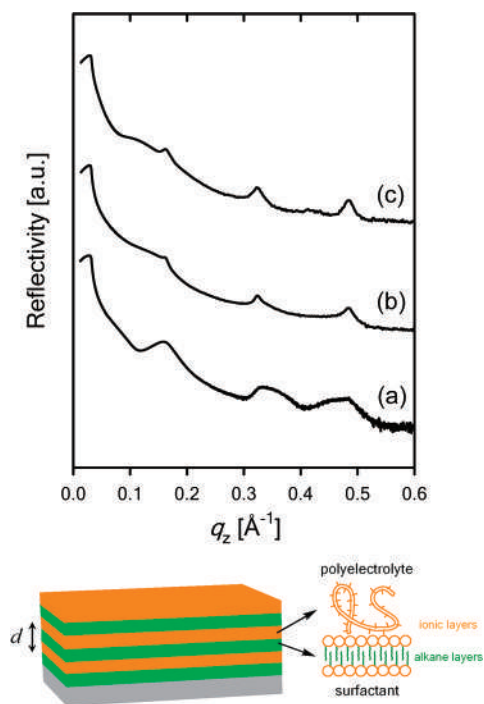
Figure 1. Top: X-ray reflectivity data for (a) PA−DS films measured under ambient conditions, (b) PA−DS−CNT films measured under ambient conditions, and (c) PA−SDS−CNT films measured at relative humidity (RH) 89%. Ambient conditions refer to $T = 298$ K and RH = 29%. Films were spin-coated on Si(100) substrates. Bottom: Schematic of polyelectrolyte−surfactant lamellar assembly. The ionic layers correspond to polyelectrolyte and SDS ionic head groups, whereas the alkane layers correspond to interdigitated hydrophobic tails (dodecyl groups). d = lamellar spacing.

Figure 2. Cyclic voltammograms corresponding to (a) 1 mM $[Fe(CN)_6]^{4-}$ and (b) 1 mM $[Ru(NH_3)_6]^{3+}$. Both experiments were carried out in buffer solution at pH 7.0; scan rate 100 mV·s^{-1}.Thin line, bare graphite electrode; bold line, electrode modified with PA−DS.

is given by the sum of the microphases. Considering the length of the dodecyl chain is 1.54 nm,[16,22] the polyelectrolyte plus ionic headgroup contributes with a thickness of 2.42 nm; this corresponds to a relatively thick layer in comparison with the results presented for self-assembled poly(acrylate)−poly(allylamine) systems at neutral pH, where very thin layers (0.3−0.5 nm) were reported for both polyelectrolytes.[23]

Electrochemical Response. Four benchmark redox probes with different characteristics were studied that take into account the electrode surface and the chemical and electrostatic characteristics of the polyelectrolyte−surfactant complex. Ferrocyanide is a negative ion and a redox system in which the electron-transfer (ET) process is surface-sensitive. Hexaammineruthenium is a positive ion and a redox system in which the ET process is carried out by an outer-sphere mechanism, without any electrocatalytic or adsorption step and a low reorganization energy. Dopamine is a positive charged species at neutral pH and a redox system in which the ET process depends on adsorption processes and proton concentration. Ascorbic acid is negatively charged at neutral pH and a redox system in which the ET process is also surface-sensitive and depends on proton concentration.[17]

It is interesting to study the electrochemical properties of $[Fe(CN)_6]^{4-}$ and $[Ru(NH_3)_6]^{3+}$ ions confined in these films because of their electrocatalytic ability to act as electron-transfer mediators for biosensors and biofuel cells. In this context, polyelectrolyte films composed of ferrocene-modified
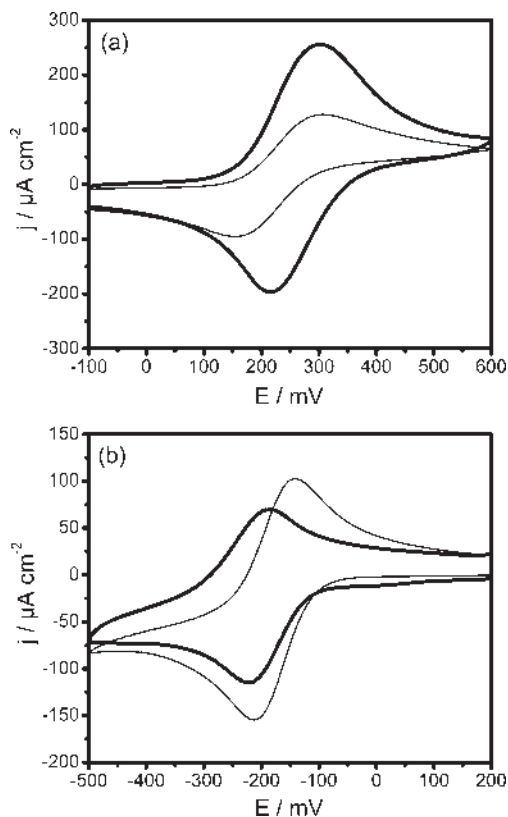
poly(amine)s and osmium complex-appended poly-(allylamine) and poly(vinylpyridine) have been used to construct mediator-type biosensors.[8,9,24−27] In these systems, the redox mediators are attached to the polymer chains to immobilize the redox center in the polyelectrolyte films because the redox compounds are often water-soluble. In these applications, it would be advantageous if redox ions such as $[Fe(CN)_6]^{4-}$ and $[Ru(NH3)_6]^{3+}$ could be retained in the films and used as an electron mediator.

The electrochemical responses of this film-coated electrode to highly charged ions, $[Fe(CN)_6]^{4-}$ and $[Ru(NH_3)_6]^{3+}$, are shown in Figure 2 , panels a and b, respectively. In both cases, the thin line corresponds to the response on bare graphite, showing the typical behavior for these couples, with $[Fe(CN)_6]^{4-}$ presenting a large peak separation ($\Delta E_p = 160$ mV), while $[Ru(NH_3)_6]^{3+}$ practically presents a reversible behavior ($\Delta E_p = 75$ mV) for cyclic voltammetry carried out at 100 mV·s^{-1}. Bold lines correspond to the current response of these redox species on the electrodes modified with PA−DS in similar conditions. They present important differences: $[Fe(CN)_6]^{4-}$ shows an increase in the current, practically doubled, and a decrease in the potential peak separation from 170 to 90 mV. This increase in current reflects the incorporation of this species into the polyelectrolyte−surfactant layer, a behavior also observed by Noguchi and Anzai[12] with multilayer polyelectrolyte films containing PA and negatively charged polysaccharides. On the other hand, the observed peak current scales with the square root of the scan rate, showing that this redox species presents
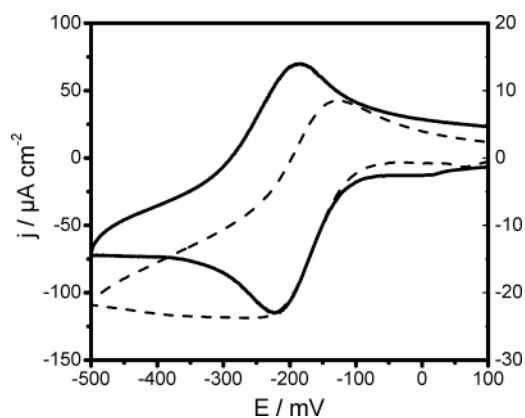
Figure 3. Cyclic voltammogram corresponding to 1 mM $[Ru(NH_3)_6]^{3+}$. Dashed line corresponds to a scan rate of 5 mV·s^{-1} (current scale at right); solid line corresponds to a scan rate of 100 mV·s^{-1} (current scale at left).

diffusional behavior inside the film; therefore the reduction in the potential peak separation can be attributed to an improvement in the rate of the electron-transfer process between ferrocyanide and the graphite surface. The apparent redox potential (determined as the average between oxidation and reduction peaks) shifts after the modification, moving from 225 to 260 mV, in agreement with the behavior observed for multilayer PA systems.[12,28]

On the other hand, in the presence of $[Ru(NH_3)_6]^{3+}$, the modified electrode shows a decrease in current and a peak separation of 23 mV (Figure 2b). This last value and the change in shape of the voltammograms, mutating from the behavior of species under semi-infinite diffusional regime to that corresponding to a thin-layer regime, indicate an important effect of this modified surface on highly charged positive redox species. Figure 3 shows the cyclic voltammograms for the modified electrode at two different scan rates. At 5 mV·s^{-1} (dashed line) a peak separation of 88 mV is observed, while for the voltammogram at 100 mV·s^{-1} (solid line) the peak separation is 23 mV. This trend in peak separation as the scan rates increase suggests that the penetration and further diffusion of $[Ru(NH_3)_6]^{3+}$ in this film is a slow process restrained by the positively charged polyelectrolyte. In the first case, the slow scan rate allows detection of the ions present in the film plus those diffusing from the solution throughout the film, while at faster scan rates the electrode is able to detect only the species confined in the film close to the electrode.

When the modified electrode is exposed to 1 mM solution of either of these ions, rinsed, and immersed in a buffer solution, it can be observed that $[Fe(CN)_6]^{4-}$ remains confined in the matrix after several cycles, while the ruthenium complex is immediately lost.

In polyelectrolyte multilayer films, the thickness affect the behavior of redox species,[12,29] and it can be regulated by changing the number of immersion steps. In the films presented here, this can be done by simply modifying the amount of complex cast on the electrode. As an example, electrodes were modified with a mass of PA—DS complex 25 times greater than the electrodes presented in Figure 2. The mass retained on the electrode surface can be compared with those presented previously by measuring the thickness of the film deposited on graphite with a stylus profilometer. For the electrodes presented in Figure 2 a film
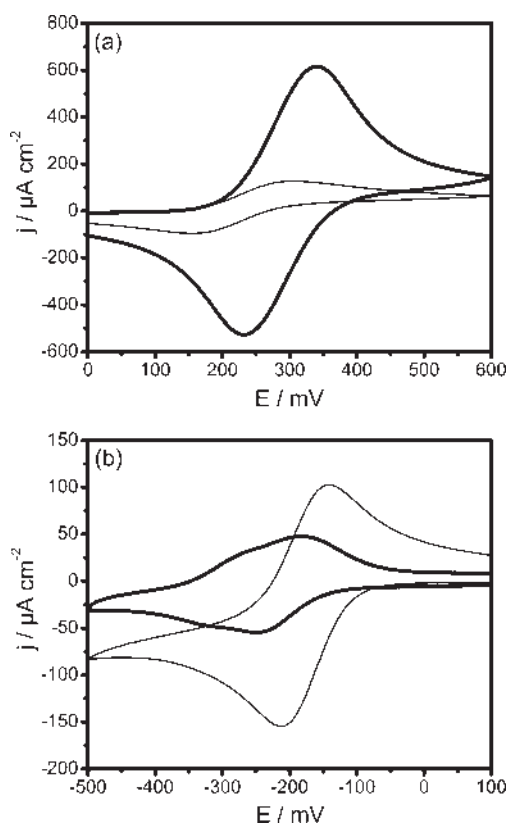

Figure 4. Cyclic voltammetries for (a) ferrocyanide and (b) hexaamineruthenium at a bare graphite electrode (thin line) and at a modified PA—DS graphite electrode (bold line). Experimental details are given in the text.

of 2 μm thickness was observed, while for the new ones the film adopts a concave shape with a height of 20 μm at the center and 60 μm at the border, reflecting an important difference in the amount of complex cast on the graphite surface. This change in the film thickness shows a striking effect on the behavior of the electroactive ions and their confinement into the film. Figure 4 shows the cyclic voltammograms for the thicker electrodes. The voltammogram for $[Fe(CN)_6]^{4-}$ shows several differences (Figure 4a): the current is around 5 times higher than for the bare graphite electrode, peak separation is practically the same (120 mV), and the apparent redox potential is shifted from 225 to 285 mV versus Ag/AgCl. Even though the signal is mainly due to the surface-confined ion in the film, the shape of the voltammogram corresponds to diffusional behavior. The same type of modified electrode exposed to $[Ru(NH_3)_6]^{3+}$ shows a more complex mechanism (Figure 4b). The observed current is smaller than in the thinner film; however, here the two processes previously mentioned are evident, one related to diffusion of the ion throughout the film with an apparent redox potential ca. −200 mV and a second one corresponding to the surface-confined ion, ca. −300 mV. The differences observed in the behavior for the electrodes presented in Figures 2 and 4 are similar to those observed by Anzai and co-workers[12,29] for polyelectrolyte multilayer films (PEM). They have studied the behavior of ferrocyanide as redox probe and shown that, as PEM films get thicker, a second redox process can be observed, one corresponding to the redox ion diffusing throughout the film and the other due to the redox ion confined in the film.
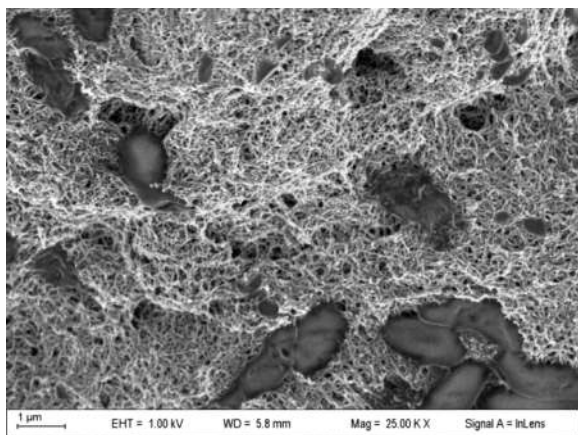
Figure 5. Micrograph of a screen-printed graphite electrode modified with PA–DS–CNT.
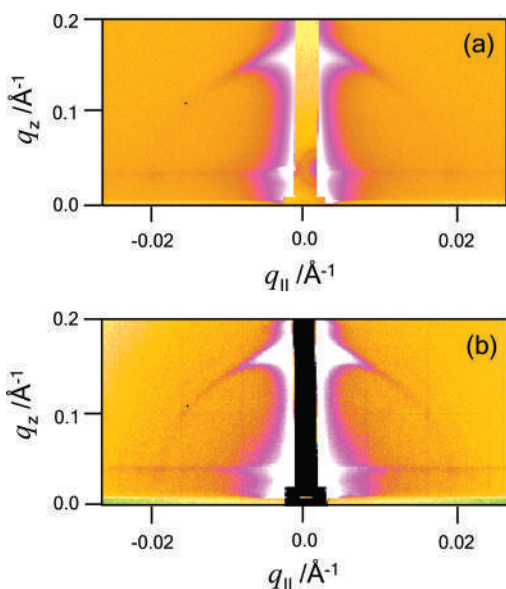

Figure 6. GISAXS patterns obtained from (a) PA–DS and (b) PA–DS–CNT films measured at an incident angle of 0.27° under ambient conditions. Films were spin-coated on Si(100) substrates.

The graphite modified electrodes were tested with other two probes of great interest in biomedical sciences, ascorbic acid and dopamine. For both couples, the oxidation on carbon is a surface-sensitive process. McCreery[17] has established a further differentiation: dopamine requires adsorption to show an effective electron-transfer process, while ascorbate does not.

At neutral pH, ascorbate and dopamine exist in different ionic forms. Ascorbate is an anion (pK_a = 4.10) while dopamine is a cation (pK_a = 8.87). It is well-known that these species are oxidized at high overpotentials on bare graphite electrodes, and different methods has been introduced to decrease such overpotentials.[3,30−32] The modification of the surface with PA–DS slightly decreases the overpotential in which the oxidation process is observed with respect to the bare graphite electrode; however, no currents peaks are observed even at an overpotential of 200 mV.

CNT Incorporation. As sodium dodecyl sulfate is frequently used to disperse carbon nanotubes (CNT) in aqueous solutions,[33,34] and
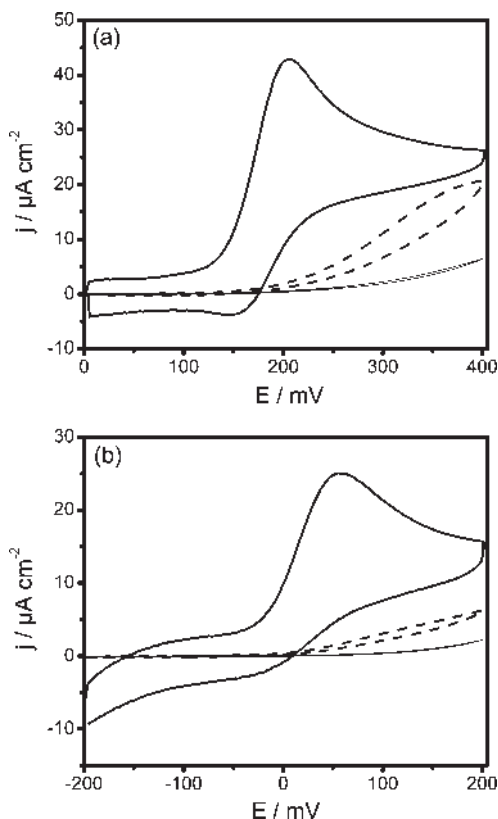

Figure 7. Cyclic voltammetry for (a) dopamine and (b) ascorbate at a bare graphite electrode (thin line), at a PA–DS-modified electrode (dashed line), and at a PA–DS–CNT-modified graphite electrode (bold line). Experimental details are given in the text.

in turn CNT show excellent electrocatalytic properties, we decided to investigate whether polyelectrolyte–surfactant matrix could be useful to disperse and retain the CNT at an electrode surface. Figure 5 shows a micrograph of this modified electrode. It can be observed that CNT are evenly distributed throughout the surface, revealing that CNT are efficiently entrapped within the polymeric net and homogeneously distributed on the electrode surface.

The structure of the whole film was investigated by X-ray reflectivity. The results show that the presence of carbon nanotubes dispersed in the PA–DS film perturbs neither the presence of lamellar structures nor the lamellar spacing [Figure 1 (top), trace b]. To further investigate the structural characteristics of PA–DS–CNT thin films, XRR measurements were performed under controlled humidity conditions. The aim of these experiments was to corroborate whether the presence of humid/aqueous environments promote drastic changes in the film mesostructure due to swelling of the polyelectrolyte domains. Figure 1 (top), trace c, depicts XRR data for PA–DS–CNT films in humid conditions (RH ∼ 89%). It is evident that the humid environment does not alter the lamellar structuring of the film.

Using GISAXS with an incident angle of 0.27°, we observed similar scattering patterns for the lamellar PA–DS and PA–DS–CNT films (Figure 6). The pronounced diffuse Bragg peak observed for both films in the direction normal to the substrate describes the same lamellar spacing as that observed by X-ray reflectivity.
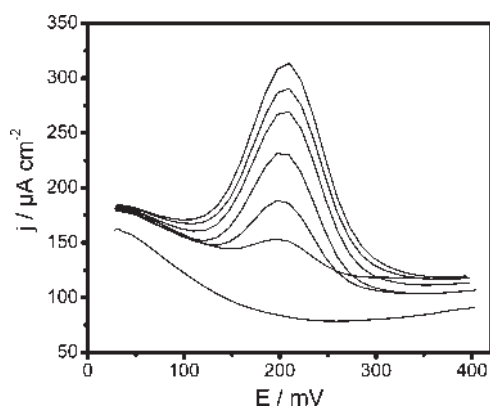
Figure 8. Differential pulse voltammetry for a dopamine in a 50 mM N-(2-hydroxyethyl)piperazine-N'-2-ethanesulfonic acid (HEPES; pH 7.0) buffer solution at different concentrations: 0, 2.5, 10, 25, 50, 75, and 100 μM (peak current increases as concentration increases).

Figure 9. Differential pulse voltammetry for a mixture containing 10 μM dopamine and 1 mM ascorbate in a 50 mM HEPES (pH 7.0) buffer solution.

These results suggest that the PA—DS—CNT films consist of slightly misaligned microdomains, having well-oriented lamellar structures in its own microdomains. The misalignment in the vertical direction leads to GISAXS patterns consistent with that in the X-ray reflectivity profiles measured previously.

PA—DS—CNT Electrochemical Response. The amperometric response of dopamine on the CNT-modified electrode shows a current higher than expected for a planar electrode, and a well-defined peak is observed even at neutral pH (Figure 7a, bold line), that cannot be observed on a PA—DS-modified electrode (Figure 7a, dashed line). The electrochemical oxidation process of dopamine is a complex one, involving two electrons and two protons, with a further follow-up ring closure reaction of the produced quinone;[35,36] therefore a smaller current response is observed for the reduction signal during the reverse cycle. However, in comparison with results obtained on a bare graphite electrode (thin line in Figure 7a) and other types of surfaces, at this pH, the oxidation potential achieved is one of the lowest, evidencing an efficient adsorption mechanism allowing dopamine to react faster at this modified surface.

In the case of ascorbate (Figure 7b, bold line), a well-shaped peak is observed close to the formal potential, in clear contrast to the bare graphite electrode (Figure 7b, thin line).[31] The improvements observed with respect to the bare graphite and the PA—DS electrodes are a reflection of the good dispersion and connectivity of the CNT in the polyelectrolyte—surfactant matrix.

Analytical Applications. Quantification of both species can be carried out by either cyclic voltammetry or differential pulse voltammetry. For cyclic voltammetry at a scan rate of $10\,\mathrm{mV\cdot s^{-1}}$, both species present an amperometric linear response as the concentration increases. For dopamine, the calibration curve presents a linear range from 10 to 200 μM with a sensitivity of 71 nA$\cdot\mu$M^{-1} and a detection limit of 6 μM, calculated on the basis of 3σ (σ being the residual standard deviation of the intercept). By the same method, ascorbate shows a linear range between 25 and 200 μM, with a sensitivity of 40 nA$\cdot\mu$M^{-1}, practically half the sensitivity for dopamine. The difference in sensitivity can be attributed to a different number of electrons involved in the oxidation process; recently, Bartlett and co-workers[37] have observed in poly(a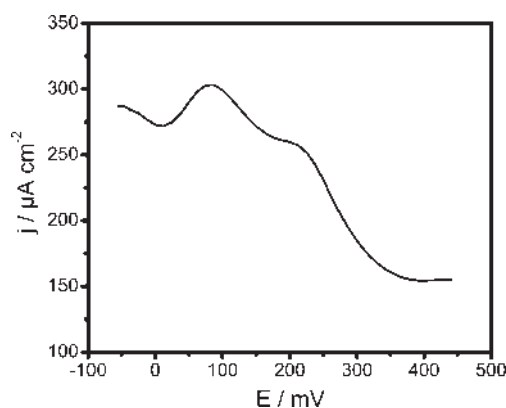niline)-modified electrodes with different anionic polyelectrolytes that the number of electrons involved in ascorbate oxidation can be one or two.

The difference in the oxidation mechanism is even more evident when a faster technique is used, for example, differential pulse voltammetry. In this case dopamine shows the typical bell-shaped signal, allowing its clear detection at a concentration of 2.5 μM (Figure 8). The calibration curve shows linear behavior at low concentrations and then levels off. Duvall and McCreery[38] have proposed as mechanism for dopamine oxidation on carbon surfaces a catalytic step in which dopamine itself can adsorb on the surface to permit "self-catalysis" by hydrogen bonding to catechols in solution undergoing oxidation, catalyzing one or more of the steps in the scheme of squares (HeHe), thus accelerating the overall redox process. This adsorption process may explain the tendency of the amperometric signal to level off at relatively low concentrations.

On the other hand, ascorbate shows a very poor signal even at concentrations of 1 mM, making possible to detect dopamine at a concentration 100 times smaller, as shown in Figure 9.

■ DISCUSSION AND CONCLUSIONS

The diffusion of charged probe ions such as $[\mathrm{Fe(CN)_6}]^{4-}$ and $[\mathrm{Ru(NH_3)_6}]^{3+}$ have been widely studied to characterize the structure of polyelectrolyte multilayer films. These films, built by layer-by-layer deposition, can growth linearly, giving a compact film, or exponentially, producing a loosely packed film. They show important differences regarding the binding and diffusion of charged ions: while the penetration of $[\mathrm{Fe(CN)_6}]^{4-}$ in compact films depends on the charge of the outer layer of the film, the exponentially grown film allows its diffusion regardless of the outer layer.[12]

The diffusion of these ions in polyelectrolyte—surfactant films shows behavior closer to that of a compact film; here the incorporation or rejection of an ion is given by the charge of the polyelectrolyte, working as a scaffold of the system, a hypothesis supported by XRR and GISAXS results. Also, the XRR experiment carried out in a humid environment (RH 89%), showing no changes regarding the lamellar structure, confirms the formation of a stable system.

In our case, poly(allylamine), positively charged, shows an important capacity to concentrate ferrocyanide (Figure 2 a) and some rejection toward $[\mathrm{Ru(NH_3)_6}]^{3+}$ (Figure 2 b). These results are more evident when the films, after being exposed

to the ion solutions, are immersed in a pH 7.0 buffer solution. A stable response is obtained in the case of the modified $[Fe(CN)_6]^{4-}$ electrode with a loading dependent on the film thickness, while in those electrodes modified with $[Ru(NH_3)_6]^{3+}$, the ion is immediately leached out. The confinement of a redox probe in the matrix can find applications in electrocatalysis or for developing mediator-type chemical sensors and biosensors.[12]

The results obtained with ascorbate and dopamine as probes do not show an important improvement in the kinetics of the oxidation process, even though SDS has shown interesting properties for the catalytic oxidation of dopamine and rejection for ascorbate as part of carbon paste electrodes.[3] It is apparent from the results shown here and those in ref 3 that a close interaction between surfactant and carbon surface should exist to observe an efficient electrocatalytic process.

On the other hand, the ability of SDS to disperse carbon nanotubes allowed introduction of a kind of material with good electrocatalytical properties. The introduction of CNT in the system does not perturb the lamellar structure of the complex, even though the intensity of the Bragg peaks in Figure 1b decreases, indicating that the propagation of the lamellar domains is somewhat smaller. The good dispersion observed in Figure 5 is clear evidence that the polyelectrolyte—surfactant complex works as a supramolecular glue that maintains the CNT attached to the graphite electrode. The introduction of CNT has a catalytic effect in the electrochemical response for dopamine and ascorbate, even though some differences are observed regarding the oxidation process when a fast technique such as differential pulse voltammetry is applied.

This study introduces a new composite material that can be easily handled and applied on graphite surfaces, with the ability to spontaneously form lamellar mesostructures on a surface. The combination of a weak polyelectrolyte bearing a primary amino group and a surfactant opens the possibility to develop more sophisticated structures in the future. Here, exploiting the ability of SDS to disperse nanoparticles, the incorporation of CNT was successfully presented, and preliminary results show that the same can be made with gold nanoparticles. On the other hand, poly(allylamine) partially modified with an osmium complex also generates a stable material combined with SDS, with interesting electrochemical properties;[39] currently, work is in progress to further characterize these new systems.

This new composite material endows electrodes with electrochemical properties distinct from those of the bare ones, and it may represent a new electrochemical system that is reasonably envisaged to be useful for electrochemical sensors and other applications, such as electrocatalysis and protein electrochemistry,

■ AUTHOR INFORMATION

Corresponding Author
*E-mail: battagli@qi.fcen.uba.ar. Fax: 54-11-45763348. Telephone: 54-11-45763378.

■ ACKNOWLEDGMENT

is a full professor at Universidad Nacional del Noroeste de Buenos Aires, Argentina.

■ REFERENCES

(1) Wang, J.; Zeng, B.; Fang, C.; Zhou, X. *J. Electroanal. Chem.* **2000**, *484*, 88.
(2) Wang, X. G.; Wu, Q. S.; Liu, W. Z.; Ding, Y. P. *Electrochim. Acta* **2006**, *52*, 589.
(3) Zheng, J.; Zhou, X. *Bioelectrochemistry* **2007**, *70*, 408.
(4) Tasis, D.; Tagmatarchis, N.; Bianco, A.; Prato, M. *Chem. Rev.* **2006**, *106*, 1105.
(5) Zhang, J.; Gao, L. *Mater. Lett.* **2007**, *61*, 3571.
(6) Mao, X.; Ma, Y.; Zhang, A.; Zhang, L.; Zeng, L.; Liu, G. *Anal. Chem.* **2009**, *81*, 1660.
(7) Deng, J. P.; Wu, C.; Yang, C. H.; Mou, C. Y. *Langmuir* **2005**, *21*, 8947.
(8) Gregg, B. A.; Heller, A. *Anal. Chem.* **1990**, *62*, 258.
(9) Danilowicz, C.; Corton, E.; Battaglini, F. *J. Electroanal. Chem.* **1998**, *445*, 89.
(10) O'Mullane, A. P.; Macpherson, J. V.; Unwin, P. R.; Cervera-Montesinos, J.; Manzanares, J. A.; Frehill, F.; Vos, J. G. *J. Phys. Chem. B* **2004**, *108*, 7219.
(11) Calvo, E. J.; Battaglini, F.; Danilowicz, C.; Wolosiuk, A.; Otero, M. *Faraday Discuss.* **2000**, *116*, 47.
(12) Noguchi, T.; Anzai, J. I. *Langmuir* **2006**, *22*, 2870.
(13) Thünemann, A. F.; Müller, M.; Dautzenberg, H.; Joanny, J. F.; Löwen, H. *Adv. Polym. Sci.* **2004**, *166*, 113.
(14) Zhou, S.; Burger, C.; Chu, B. *J. Phys. Chem. B* **2004**, *108*, 10819.
(15) Thünemann, A. F.; General, S. *J. Controlled Release* **2001**, *75*, 237.
(16) Antonietti, M.; Conrad, J.; Thünemann, A. *Macromolecules* **1994**, *27*, 6007.
(17) McCreery, R. L. *Chem. Rev.* **2008**, *108*, 2646.
(18) Priano, G.; González, G.; Günther, M.; Battaglini, F. *Electroanalysis* **2008**, *20*, 91.
(19) Kobayashi, S.; Tokunoh, M.; Saegusa, T.; Mashio, F. *Macromolecules* **1985**, *18*, 2357.
(20) Chen, W.; McCarthy, T. J. *Macromolecules* **1997**, *30*, 78.
(21) Thünemann, A. F. *Prog. Polym. Sci. (Oxford)* **2002**, *27*, 1473.
(22) Cheng, Z.; Ren, B.; Zhao, D.; Liu, X.; Tong, Z. *Macromolecules* **2009**, *42*, 2762.
(23) Shiratori, S. S.; Rubner, M. F. *Macromolecules* **2000**, *33*, 4213.
(24) Scodeller, P.; Flexer, V.; Szamocki, R.; Calvo, E. J.; Tognalli, N.; Troiani, H.; Fainstein, A. *J. Am. Chem. Soc.* **2008**, *130*, 12690.
(25) Narváez, A.; Suárez, G.; Popescu, I. C.; Katakis, I.; Domínguez, E. *Biosens. Bioelectron.* **2000**, *15*, 43.
(26) Rusling, J. F.; Forster, R. J. *J. Colloid Interface Sci.* **2003**, *262*, 1.
(27) Scodeller, P.; Carballo, R.; Szamocki, R.; Levin, L.; Forchiassin, F.; Calvo, E. J. *J. Am. Chem. Soc.* **2010**, *132*, 11132.
(28) Zahn, R.; Boulmedais, F.; Vörös, J.; Schaaf, P.; Zambelli, T. *J. Phys. Chem. B* **2010**, *114*, 3759.
(29) Wang, B.; Anzai, J. I. *Langmuir* **2007**, *23*, 7378.
(30) Cao, X.; Luo, L.; Ding, Y.; Zou, X.; Bian, R. *Sens. Actuators, B* **2008**, *129*, 941.
(31) Heras, J. Y.; Giacobone, A. F. F.; Battaglini, F. *Talanta* **2007**, *71*, 1684.
(32) Bonastre, A. M.; Bartlett, P. N. *Anal. Chim. Acta* **2010**, *676*, 1.
(33) Sinani, V. A.; Gheith, M. K.; Yaroslavov, A. A.; Rakhnyanskaya, A. A.; Sun, K.; Mamedov, A. A.; Wicksted, J. P.; Kotov, N. A. *J. Am. Chem. Soc.* **2005**, *127*, 3463.
(34) Islam, M. F.; Rojas, E.; Bergey, D. M.; Johnson, A. T.; Yodh, A. G. *Nano Lett.* **2003**, *3*, 269.
(35) Tse, D. C. S.; McCreery, R. L.; Adams, R. N. *J. Med. Chem.* **1976**, *19*, 37.
(36) Clolkowski, E. L.; Maness, K. M.; Cahill, P. S.; Wightman, R. M.; Evans, D. H.; Fossel, B.; Amatore, C. *Anal. Chem.* **1994**, *66*, 3611.

8017

dx.doi.org/10.1021/ac202213t |*Anal. Chem.* 2011, 83, 8011–8018

(37) Bonastre, A. M.; Sosna, M.; Bartlett, P. N. *Phys. Chem. Chem. Phys.* **2011**, *13*, 5365.

(38) Duvall, S. H.; McCreery, R. L. *J. Am. Chem. Soc.* **2000**, *122*, 6759.

(39) Cortez, M. L.; González, G. A.; Battaglini, F. *Electroanalysis* **2011**, *23*, 156.